ESA CONTRACT REPORT

Contract Report to the European Space Agency

Evaluation of radar altimeter path delay using ECMWF pressure-level and model-level fields

Author: Saleh Abdalla

A report for ESA contract 21519/ 08/ I-OL (CCN2)

European Centre for Medium-Range Weather Forecasts
Europäisches Zentrum für mittelfristige Wettervorhersage
Centre européen pour les prévisions météorologiques à moyen terme

ECMWF

Series: ECMWF - ESA Contract Report

A full list of ECMWF Publications can be found on our web site under:

http://www.ecmwf.int/publications/

European Centre for Medium Range Weather Forecasts
Shinfield Park, Reading, RG2 9AX, England

Contract Report to the European Space Agency

Evaluation of radar altimeter path delay using ECMWF pressure-level and model-level fields

Author: Saleh Abdalla

A report for ESA contract 21519/08/I-OL (CCN2)

European Centre for Medium-Range Weather Forecasts
Shinfield Park, Reading, Berkshire, UK

October 2013

Table of Contents

Abbreviations

AN ..... ANalysis
DTC ..... Dry Tropospheric Correction
ECMWF ..... European Centre for Medium-range Weather Forecasts
ENVISAT ..... ENVIronmental SATellite
ERS ..... European Remote sensing Satellite
ESA ..... European Space Agency
EUMETSAT ..... EUropean organization for the exploration of METeorological SATellites
FC ..... ForeCast
GB ..... Giga (1 billion) Byte
GRIB ..... GRIdded Binary
IFS ..... ECMWF Integrated Forecast System
MARS ..... Meteorological Archival and Retrieval System
MB ..... Mega (1 million) Byte
ML ..... Model Level (field)
MWR ..... Microwave Radiometer
NASA ..... National Aeronautics and Space Administration (of the United States)
NWP ..... Numerical Weather Prediction
PL ..... Pressure Level (field)
RA ..... Radar Altimeter
RHS ..... Right-Hand Side
RA-2 ..... (ENVISAT) Radar Altimeter-2
TRMM ..... Tropical Rainfall Measuring Mission
UTC ..... Coordinated Universal Time
WTC ..... Wet Tropospheric Correction

Abstract

Estimation of the path delay of the altimeter radar signal due to the existence of dry and wet (due to water vapour) air is very important to compensate for it in the sea surface height measurements. Atmospheric fields produced from numerical weather prediction models are usually used to perform this. The difference between using the model fields at native model levels versus the use of the vertically interpolated fields at ~25 constant-pressure levels is examined. For the dry component of the path delay, the difference is negligible. In the case of the wet component, the differences cannot be ignored. Therefore, the use of pressure level fields for wet path delay cannot be recommended. For the reduction of data volume and computational costs, the fields at the lowest ~60% of model levels are sufficient for the wet delay computations with negligible differences compared to the use of all levels.

1. Introduction

Estimation of the path delay of the altimeter radar signal due to the existence of the atmosphere is very important to compensate for it in the sea surface height measurements by radar altimeters. This delay can be composed into two components: dry and wet. The former is due to the existence of the (dry) air while the latter is due to the existence of the atmospheric water vapour. The wet path delay can be estimated using microwave radiometers that are typically installed together with the radar altimeter (MWR) on the same platform (e.g. Envisat and Jason satellites). Another way to estimate the wet delay is by using atmospheric fields produced from numerical weather prediction (NWP) models. This is usually favoured due to its availability. Some low-cost satellite missions lack the MWR facility (e.g. Cryosat-2) and therefore rely on model estimations.

The ECMWF Integrated Forecast System (IFS), as any other NWP model, implements a horizontal global grid of few (~2) millions of grid points, discretizes the atmospheric column into few 10's of layers (91 levels until 24 June 2013 and 137 afterwards). The use of the model fields given at all the model-levels should reproduced all the atmospheric features resolvable by the model. However, there are few practical limiting factors that may prevent the use of the model-level (ML) fields. Each atmospheric parameter (e.g. temperature) represented on the 91 ML fields (typically produced every 3 hours in the forecast, FC, and every 6 hours in the analysis, AN) occupy about 400 MB. With the increase of model levels and in the near future the horizontal resolution, this number can go up to about 2 GB/parameter/FC time step/analysis cycle. Typically, for the computations of the delay path ESA needs fields for ~2 parameters, ~16 FC time steps and 2 analysis cycles each day which may result in a daily data transfer volume of about 125 GB (note these are rough estimates and should not be quoted for any data requests). The other implication of the use of the ML fields is the need to maintain any application that uses such fields in case of change of model resolutions.

An attractive solution is the use of what is called "pressure-level" (PL) fields. The NWP usually post-processes the ML fields to represent them at limited number of levels (~25) of equal pressure. This is a standard meteorological practice for the purpose of providing easy computational environment and for standard comparisons and verifications. A procedure that implements PL field can be maintenance-free as it is not affected by changes of model vertical resolution. However, this comes at

a cost of loss of some details. The impact of using PL fields to estimate the altimeter path delay corrections is assessed against the use of ML fields.

2. Mathematical Formulations

The delay path of the altimeter radar signal, δh, due to the existence of the atmosphere can be estimated using the integration:

$$\delta h = \int_{Z_s}^{Z_a} (n_r - 1)\,\mathrm{d}z \tag{1}$$

where n_r is the refractive index of radio waves in air at ambient conditions, Z_s and Z_a are altitudes of the earth surface and the altimeter, respectively, and z is the vertical direction. n_r, which is varies along the z direction, can be written in terms of the refractivity, N_r, of radio waves in air at ambient conditions, defined as:

$$N_r \equiv (n_r - 1) \times 10^{-6} \tag{2}$$

Neglecting non-ideal gas effects, the refractivity of air can be approximated as:

$$N_r = k_1 \frac{P_d}{T} + k_2 \frac{e}{T} + k_3 \frac{e}{T^2} \tag{3}$$

where P_d and e are the partial pressure of dry air and water vapour, respectively, in hPa, T is the temperature in K and k_1, k_2 and k_3 are empirical coefficients. Rüeger (2002) provide an extensive discussion regarding various forms of Eq. (3) and the numerical values of the empirical coefficients. Here, the following specific values are used (Rüeger, 2002):

$$k_1 = 77.689\ \mathrm{K \times hPa^{-1}}, k_2 = 71.2952\ \mathrm{K \times hPa^{-1}} \text{and} k_3 = 3.75463 \times 10^5\ \mathrm{K^2 \times hPa^{-1}} \tag{4}$$

The partial pressure of dry air and water vapour are not readily available from IFS. The dry air and the water vapour are assumed to follow the ideal gas law; therefore, it is possible to write:

$$\frac{P_d}{\rho_d} = \frac{R\ T}{M_d} \tag{5}$$

$$\frac{e}{\rho_w} = \frac{R\ T}{M_w} \tag{6}$$

where ρ_d and ρ_w are the densities of the dry air and water vapour, respectively; M_d and M_w are the molar masses of dry air ($\approx 28.9644 \times 10^{-3}$ kg) and water vapour ($\approx 18.0152 \times 10^{-3}$ kg), respectively; and R is the universal gas constant (≈ 8.31434 J·mole^{-1}·K^{-1}).

It is now possible to write the refractivity of air, Eq. (3) as:

$$N_r = k_1 R \frac{\rho_d}{M_d} + k_2 R \frac{\rho_w}{M_w} + k_3 \frac{e}{T^2} \tag{7}$$

By realizing that the density of moist air, ρ, is the sum of the densities of dry air and water vapour, it is possible to write Eq. (7) as:

$$N_r = k_1 R \frac{\rho}{M_d} + \left(k_2 - k_1 \frac{M_w}{M_d} \right) \frac{e}{T} + k_3 \frac{e}{T^2} \tag{8}$$

Introducing Eq. (2) and Eq. (8) into Eq. (1) gives the following result for the path delay:

$$\delta h = 10^{-6} \times \left[k_1 \frac{R}{M_d} \int_{Z_s}^{Z_a} \rho \, dz + \left(k_2 - k_1 \frac{M_w}{M_d} \right) \int_{Z_s}^{Z_a} \frac{e}{T} dz + k_3 \int_{Z_s}^{Z_a} \frac{e}{T^2} dz \right] \tag{9}$$

The first term on the RHS of Eq. (9) is due to the density of air and is usually called the dry tropospheric correction, δh_{dry}. The remaining part of Eq. (9) is function of water vapour partial pressure and therefore is usually called wet tropospheric correction, δh_{wet}.

The hydrostatic equilibrium approximation can be used to relate air density to pressure gradient as follows:

$$\frac{dP}{dz} = -\rho g \tag{10}$$

Here, g is the acceleration due to gravity. Note that P, ρ and g are all functions of z. Therefore, it is possible to write for δh_{dry} (first term of Eq. 9):

$$\delta h_{dry} = 7.7689 \times 10^{-5} \frac{R}{M_d} \int_0^{P_s} g^{-1} \, dP \tag{11}$$

with P_s is the atmospheric surface pressure.

The acceleration due to gravity that was given by the World Geodetic System 1984 (WGS 84), can be approximated as a function of latitude and altitude as follows:

$$g = g_o - 2.59296 \times 10^{-2} \cos(2\phi) + 5.67 \times 10^{-5} \cos^2(2\phi) - 3.086 \times 10^{-6} z \tag{12}$$

where ϕ is the latitude, z is the altitude in km and $g_o = 9.80620$ m·s^{-2}.

The wet tropospheric correction, i.e. the second and the third terms of Eq. (9), can be written by inserting the numerical values of Eq. (4) as:

$$\delta h_{wet} = \left(7.12952 - 7.7689 \frac{M_w}{M_d} \right) \times 10^{-5} \int_{Z_s}^{Z_a} \frac{e}{T} dz + 0.375463 \int_{Z_s}^{Z_a} \frac{e}{T^2} dz \tag{13}$$

3. Numerical Computations

In order to compute the integrations in Eq. (11) and Eq. (12), the following issues need to be sorted out:

- The choice of the numerical scheme for the integration.
- Evaluation of the pressure vertical variation in the case of ML computations.
- Evaluation of the layer heights and thicknesses.
- Evaluation of the partial pressure of water vapour, e, from the fields archived at ECMWF.
- Treatment of the surface especially in the case of the PL computations when the surface intersects with pressure levels.

Trapezoidal rule is used for the numerical integration. Better integration schemes are not necessary as the aim here is to compare the results rather than computing absolute fields with higher accuracy. The limits of integration are taken to be the Earth surface and the uppermost model layer. The atmospheric contribution beyond that is negligible. This will be confirmed later.

For its computational procedures, the IFS model divides the atmosphere vertically into N_{levels} layers. At the time of the original writing, N_{levels} =91 layers and was increased on 25 June 2013 to 137 layers. These layers are defined by the pressures at the interfaces between them (the "half-levels"), and these pressures are given by (ECMWF, 2011):

$$P_{k+1/2} = A_{k+1/2} + B_{k+1/2} P_s \quad \text{for } 0 \le k \le N_{levels} \tag{14}$$

where $A_{k+1/2}$ and $B_{k+1/2}$ are constants whose values effectively define the vertical coordinate. Their numerical values are tabulated at ECMWF (2013) for all ECMWF current and past vertical model configurations. They are also available in the GRIB headers of all fields archived at model levels. The evaluation of the "full-level" pressure value associated with each layer, P_k, i.e. at the middle of the layer k, is possible using:

$$P_k = \left(P_{k-1/2} + P_{k+1/2}\right) \; / \; 2 \quad \text{for} 1 \le k \le N_{levels} \tag{15}$$

For the elevation computations, the (moist) air is assumed to follow the ideal gas law provided that the actual temperature is replaced by the virtual temperature, T_v, defined as follows:

$$T_v = T\left[1 + \left(\frac{M_d}{M_w} - 1\right) q\right] \tag{16}$$

where q is the specific humidity. The hydrostatic approximation, Eq. (10); the ideal gas law for air and the virtual temperature definition, Eq. (16), are combined to write:

$$\frac{dP}{dz} = -\frac{g M_d}{R T_v} \tag{17}$$

Eq. (17) can be integrated to find the thickness of any atmospheric layer as follows:

$$\Delta z = -\frac{R T_v}{g M_d} \ln\left(\frac{P_{k+1}}{P_k}\right) \tag{18}$$

The partial pressure of water vapour, e, is not readily available from ECMWF archives. However, it is possible to compute it using the pressure and humidity as follows:

$$e = \frac{r}{r + \frac{M_w}{M_d}} P \tag{19}$$

where r is the mixing ratio defined as:

$$r = \frac{q}{1-q} \tag{20}$$

with q being the specific humidity which is readily available from MARS.

The integration along the atmospheric column is straightforward. However, the surface needs a special treatment especially in the case of PL computations. The model levels are designed to follow the Earth surface at lower levels and, therefore, there is no intersection between the surface and the model levels. On the other hand, the case where the surface intersects with the lower pressure levels is quite common. The process of pressure-level field production, which is an interpolation of the ML fields in the upper atmosphere, becomes an extrapolation near the surface. For the purpose of evaluating Eq. (11) and Eq. (12), the surface pressure needs to be used in order to trim (or extend) the pressure fields to the surface where surface fields are also used (surface temperature and orography). Extra errors are introduced through this process. As the aim of this work is to compare between the uses of PL versus ML fields, such extra error may lead to incorrect conclusions.

To limit this impact, another approached is followed. The PL fields are linearly interpolated to the model levels and the interpolated fields are used in the evaluations of Eq. (11) and Eq. (12). With more model levels (i.e. finer ML increments) compared to pressure levels, the error associated with this procedure was found to be much lower that having to deal with the surface crossings with pressure levels (not shown here).

4. Results

The following Global operational ECMWF IFS model (T1279) fields were retrieved from the Meteorological Archival and Retrieval System (MARS):

- Temperature, T, at all model levels and at all available pressure levels.
- Specific humidity, q, at all model levels and at all available pressure levels.

- Surface pressure, P_s.
- Skin temperature, T_s.
- Geopotential height at the surface (model orography).

There are 91 model levels numbered from top with 91 being the one very close to the surface. The model fields are interpolated to the following 25 pressure levels: 1, 2, 3, 5, 7, 10, 20, 30, 50, 70, 100, 150, 200, 250, 300, 400, 500, 600, 700, 800, 850, 900, 925, 950, 1000 hPa.

The fields cover a six-month period from January to June 2012. The 24-, 30-, 36- and 42-hour forecasts from both 00 and 12 UTC analyses times on the 1st. and on the 15th. of the month were selected to achieve balance between the amount of data and the representation of the results. This selection of 96 cases accounts for the daily variation (if any) as well as the seasonal variations, to some extent. For further tests with ML fields (Section 4.3) the period was extended to cover the whole year from July 2011 to June 2012 with only forecasts from 00 UTC analyses. This selection also gave 96 cases.

4.1. Dry Tropospheric Correction

By examining Eq. (11) and Eq. (12), it is possible to note that the dependence of the dry tropospheric correction on the detailed profile of the atmosphere is very small. This was indeed confirmed by the numerical computations. The mean difference between the computations based on the PL fields and the ML fields for 96 cases during the period from 1 January to 15 June 2012 (sampled as described above) does not exceed few micrometres (μm) as can be seen in Figure 1. Individual snapshots of the differences (not shown) display slightly higher values with maxima in the order of 30 μm. The differences are mainly due to the interpolation in addition to the round-off and truncation errors.

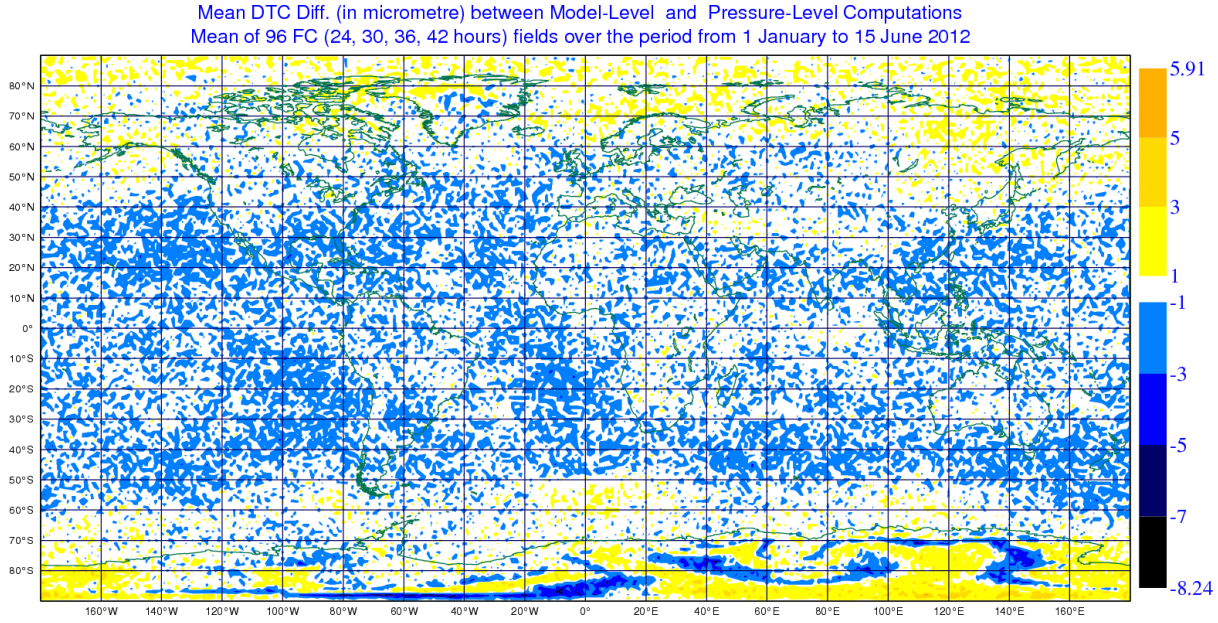

Figure 1: The mean difference in DTC between PL and ML computations in μm. The period covered is from 1 January to 15 June 2012 sampled as 4 forecast fields (24, 30, 36 and 42 hours) from 2 analysis-cycles (00 and 12 UTC) twice a month (96 cases).

4.2. Wet Tropospheric Correction

The dependence of the wet tropospheric correction of the atmospheric profile is complicated as one would expect from Eq. (13). The wet tropospheric correction for the 96 cases covering the period from 1 January to 15 June 2012 (sampled as described above) were computed using the ML fields (reference) and the PL fields. The mean difference between the two sets of computations is shown in Figure 2. The mean difference varies from -2 mm to 4.5 mm. The differences for the case of 30-hour forecast from 00 UTC on 1 January 2012 (valid at 06 UTC on 2 January) are shown in Figure 3. The differences in this typical case range from -17 mm to slightly above 20 mm. Considering the accuracy of the sea surface height measurements from radar altimeters, such differences are quite high. Most of the large differences are confined between 40°N and 40°S.

To get some sense about the reasons behind the relatively large deviations between PL and ML computations, the temperature and specific humidity profiles at several latitudes along the zero-meridian are plotted in Figure 4 for temperature and Figure 5 for humidity. It is clear from Figure 4 that the PL temperature profiles follow closely the corresponding ML profiles. Noticeable differences exist, though, near the surface and the tropopause especially in the Tropics.

The situation with the humidity profiles in Figure 5 is not as simple as for the case of temperature profiles. Humidity varies over 4 orders of magnitudes with S-shaped profiles. Nevertheless, the profiles show several irregularities especially in the Tropics. PL profiles deviate quite significantly from the corresponding ML profiles due to those irregularities. Sometimes the PL and ML profiles can be about one or more order of magnitudes different (e.g. the profiles at 20°N and at 20°S). This is the main reason behind the deviations of PL computations with respect to the ML reference.

Figure 5 suggests that the humidity at the higher levels (above ~150-200 hPa) is about 1000 times smaller than the humidity at the lower levels. This will be utilised further in Section 4.3.

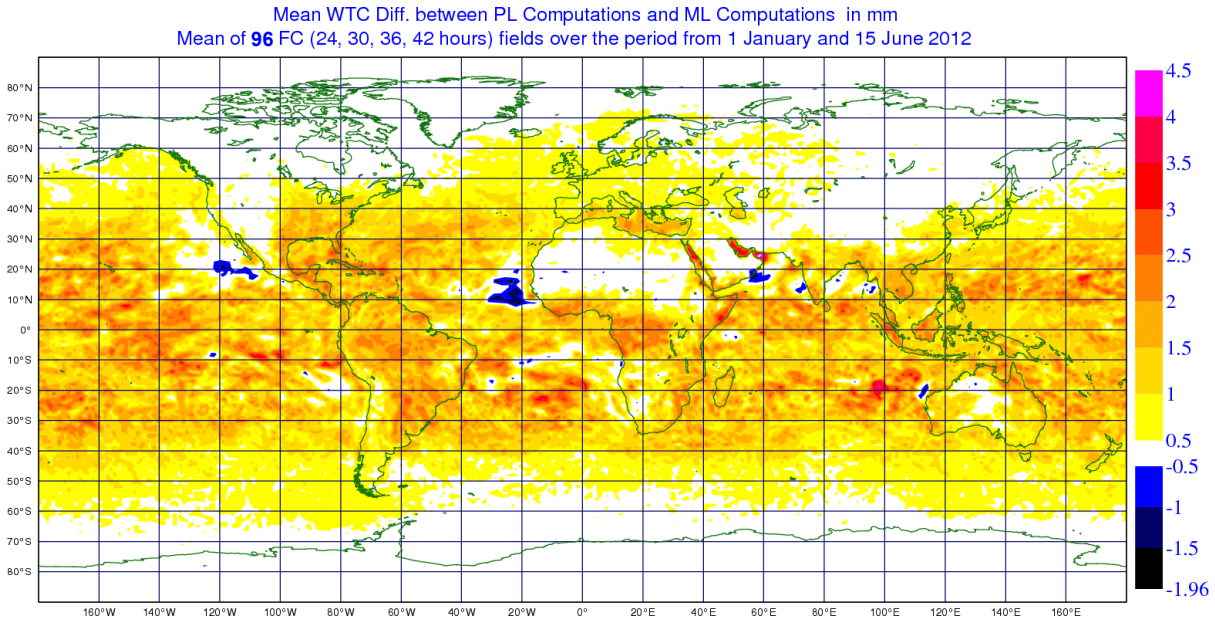

Figure 2: The mean (over 96 cases from January to July 2012) wet tropospheric correction difference between PL and ML computations in mm. The period covered and its sampling are the same as for Figure 1.

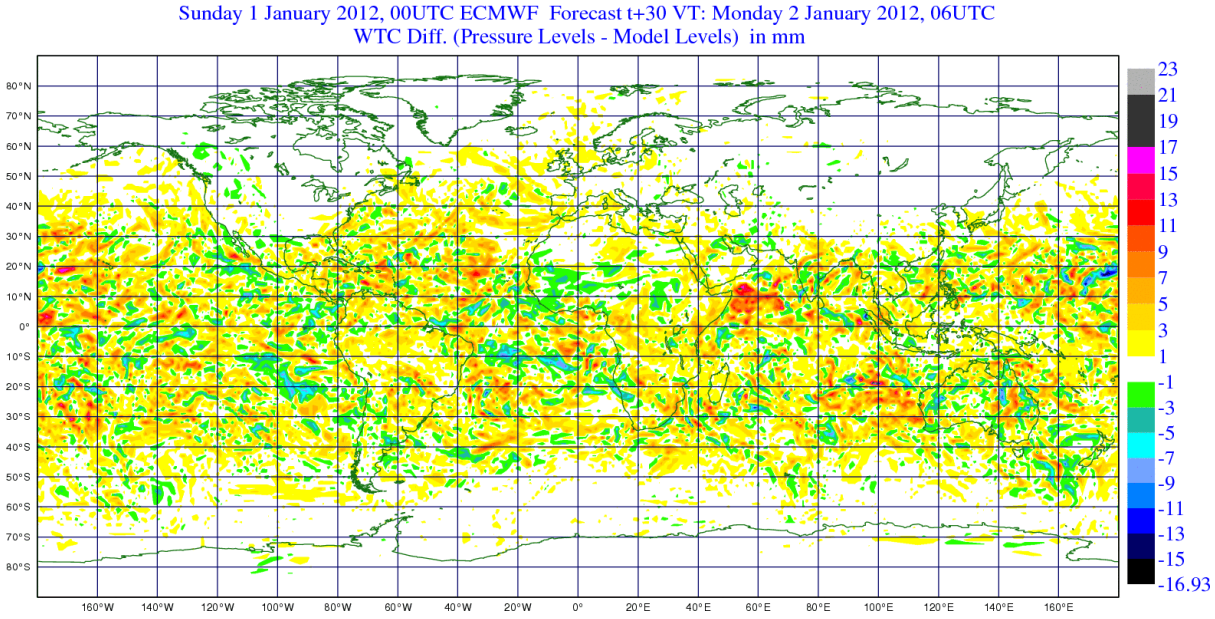

Figure 3: The WTC difference between PL and ML computations in mm for the case of 30-hour forecast from 00 UTC on 1 January 2012 (valid at 06 UTC on 2 January).

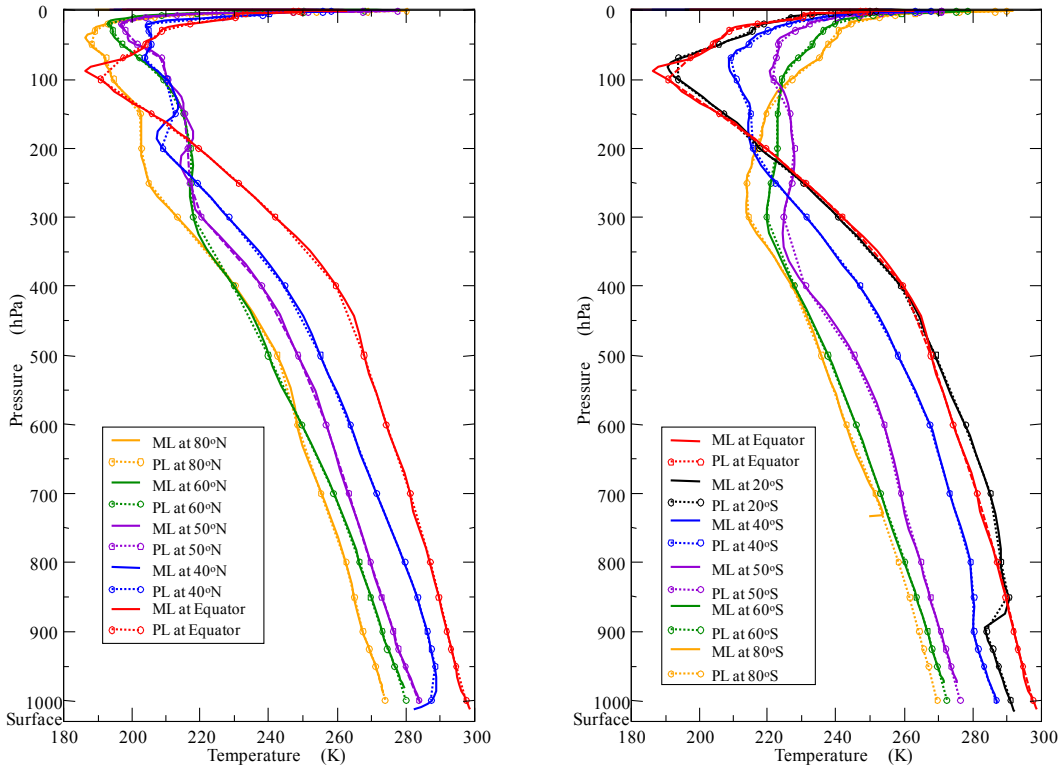

Figure 4: Temperature profiles at various latitudes along the zero-meridian for the 24-hour forecast from 00-UTC analysis on 1 January 2012. Circles on PL profiles indicate the location of the corresponding PL.

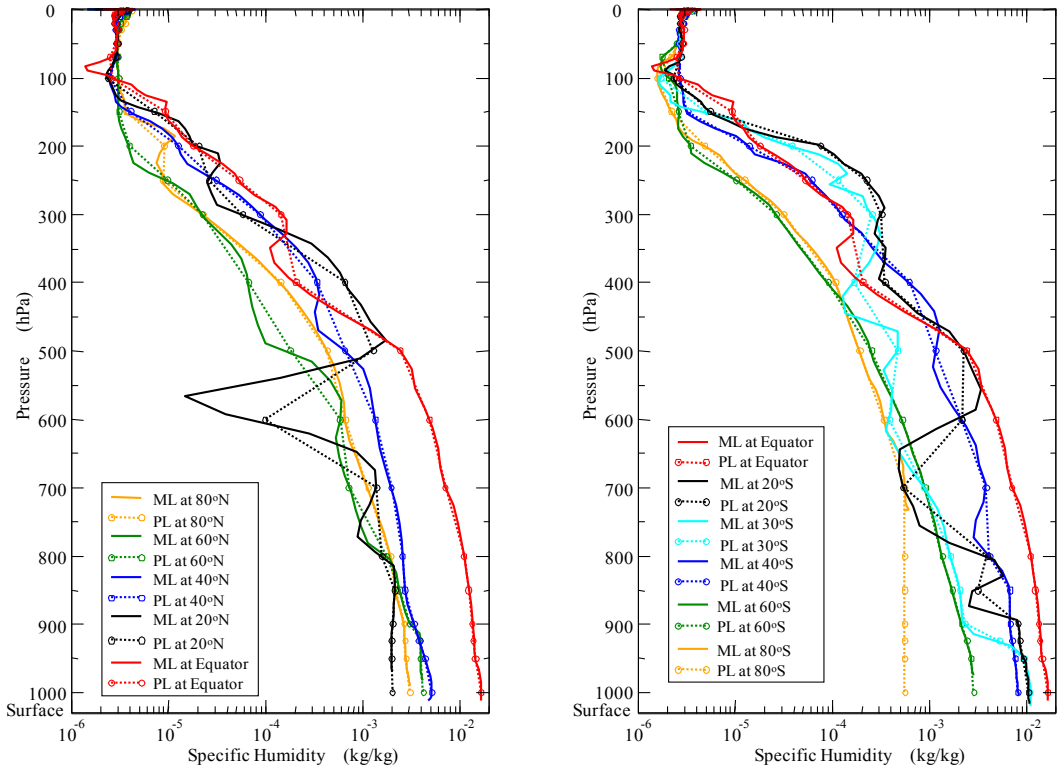

Figure 5: Specific humidity profiles at various latitudes along the zero-meridian for the 24-hour forecast from 00-UTC analysis on 1 January 2012. Circles on PL profiles indicate the location of the corresponding PL. Note the logarithmic scale of the humidity.

4.3. Are All Model Levels Needed?

It is quite clear that WTC computations based on pressure-level fields cannot reproduce the results of the model-level computations. This implies that model-level fields should be used for the accurate evaluation of the WTC. The question now is whether any savings can be achieved by reducing the number of fields used for the integration of Eq. (13).

Based on the current ECMWF model configurations (91 model levels), the mean (over the whole globe) cumulative contribution of each model layer to the integration of Eq. (13) starting from the surface is shown in Figure 6. It is clear that the contribution from layers above model level 58 is small and account, on average, for only 1% of the computed values. This corresponds to about 1.3 mm (on average). This difference may be considered as significant for radar altimeters. A smaller difference can be achieved by considering the contribution of few more layers. The overall contribution of the layers above model level 48 is less than 0.1% (~0.07mm). In other words, if the lowest 44 model levels are used to evaluate Eq. (13), the average WTC error would be around 0.07 mm (0.1%). This is supported by the fact that humidity in the upper atmosphere is quite low. For example, Figure 5 shows that humidity above ~150-200 hPa is about 1000 times smaller than the humidity in the layers below ~400-500 hPa.

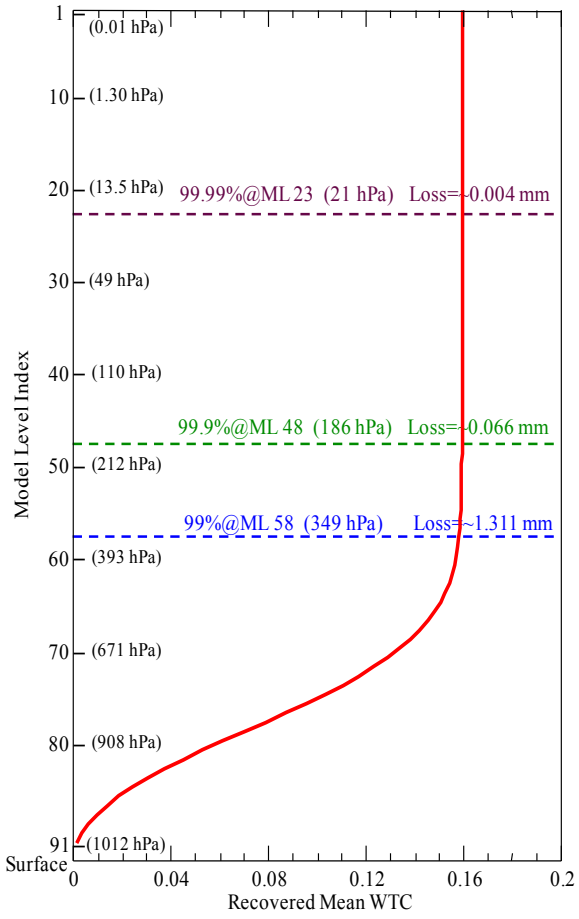

Figure 6: The global mean cumulative contribution of each model layer to the computations of the WTC starting from the surface for the current ECMWF model configuration. The pressure values at each level are based on standard conditions and given here for guidance only.

The wet tropospheric correction was computed using ML fields but the integration of Eq. (13) was carried out from the surface to ML 48 (i.e. using only the lowest 44 ML fields) over the 96 cases from July 2011 to June 2012 (sampled as described above). Figure 7 shows the mean WTC deficit (negative difference) with respect the ML computations using all 91 model levels. It is important to remember that ignoring ML fields is a kind of a truncation that leads to smaller WTC values compared to the case that includes all ML fields. Therefore, the deficit is always positive as shown in Figure 7. In the areas north of latitude 40°N and south of 30°, the mean difference is less than 0.06 mm and except for few areas in the south-eastern parts of Asia, the mean differences are below 0.1 mm. This is within the expected mean differences according to Figure 6. The maximum mean difference over the 96 cases is about 0.16 mm.

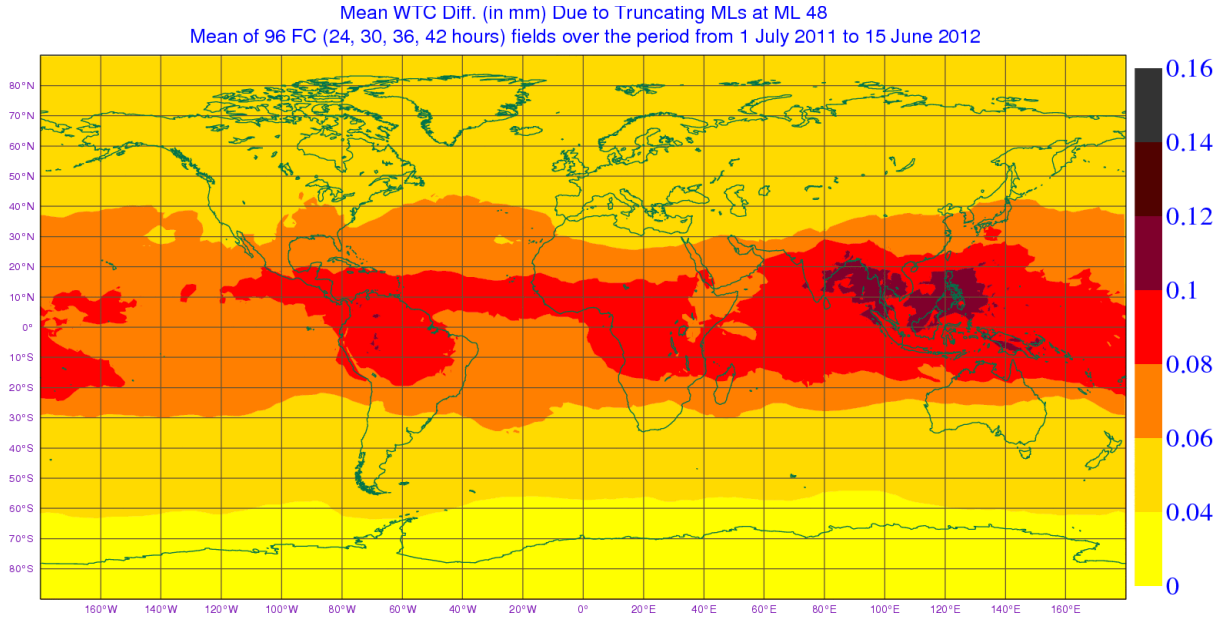

Figure 7: The mean WTC deficit (in mm) due to ignoring model levels higher than ML 48 (i.e. taking into account the lower 44 model levels only) compared to considering all 91 model levels. The period covered is from 1 July 2011 to 15 June 2012 sampled as 4 forecast fields (24, 30, 36 and 42 hours) from the analysis cycle at 00 UTC twice a month (96 cases).

The maximum difference at each of the 96 cases was extracted and plotted as a time series in Figure 8. At each date there is a cluster of 4 points for the 4 forecast fields. The maximum difference of almost all cases is well below 0.4 mm. However, the maxima in mid July 2011 are very large (as high as 7.3 mm for the 42-hour forecast from 00 UTC on 15 July). Some of the maxima in mid March are higher than the 0.4 mm limit.

The WTC deficits of the case of the highest maximum difference, which is the 42-hour forecast from 00 UTC on 15 July 2011 (valid at 18 UTC on 16 July), from truncating the integration at various model levels are shown in Figure 9 to Figure 19. In specific, the maps for deficits due to truncations at ML 40 to ML 60 with increments of 2 are shown. Ignoring all model levels above ML 42 (Figure 9 and Figure 10) resulted in differences below 0.05 mm everywhere except for two small spots in the western Pacific south of Japan where the error was below 0.1 mm. Ignoring more layers in

integrating Eq. (13), increases the areas with errors above 0.05 mm but almost none above 0.1 mm (with the exception of the two spots in Figure 9 and Figure 10) up to ML 46 (Figure 11 and Figure 12). Note the errors are mainly in the Tropics. Truncating the ML fields above ML 48 leads to WTC errors below 0.2 mm except for two areas: the first is one of the two spots that appear in Figure 9 and Figure 10 and the second is over the Himalayas (Figure 13). Figure 14 to Figure 19 show the impact of ignoring more model levels.

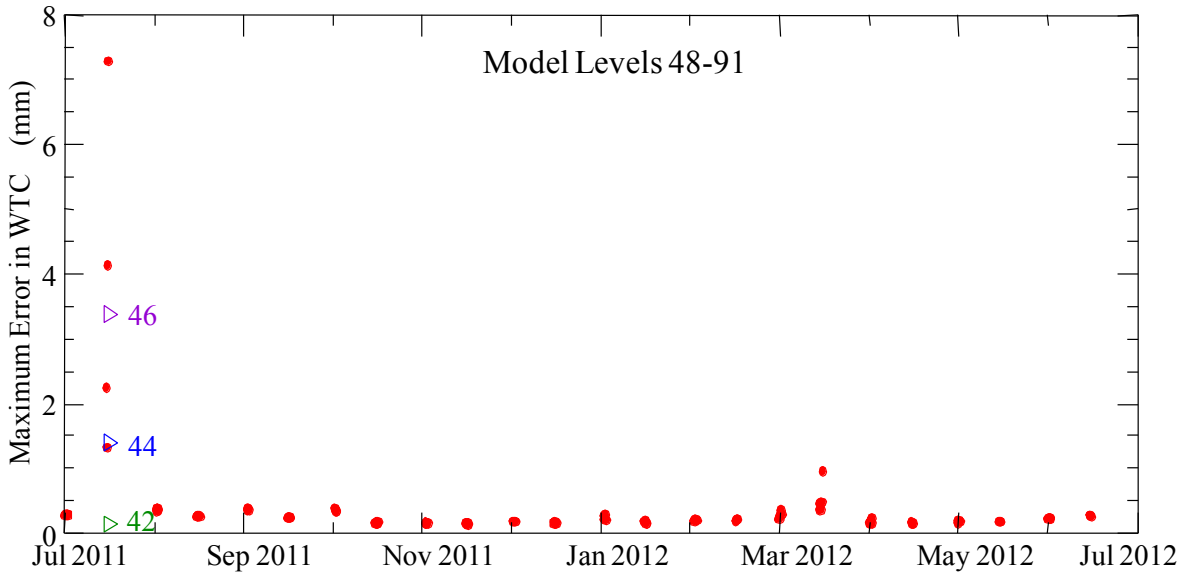

Figure 8: The maximum deficit due to truncating the WTC computations at ML 48 at each of the 96 cases from July 2011 to June 2012. Note that most of the dots are in fact a cluster or 4 dots for the 4 forecasts at that date. Triangles indicate the maximum deficit due to truncation at the model level of the number next to the triangle.

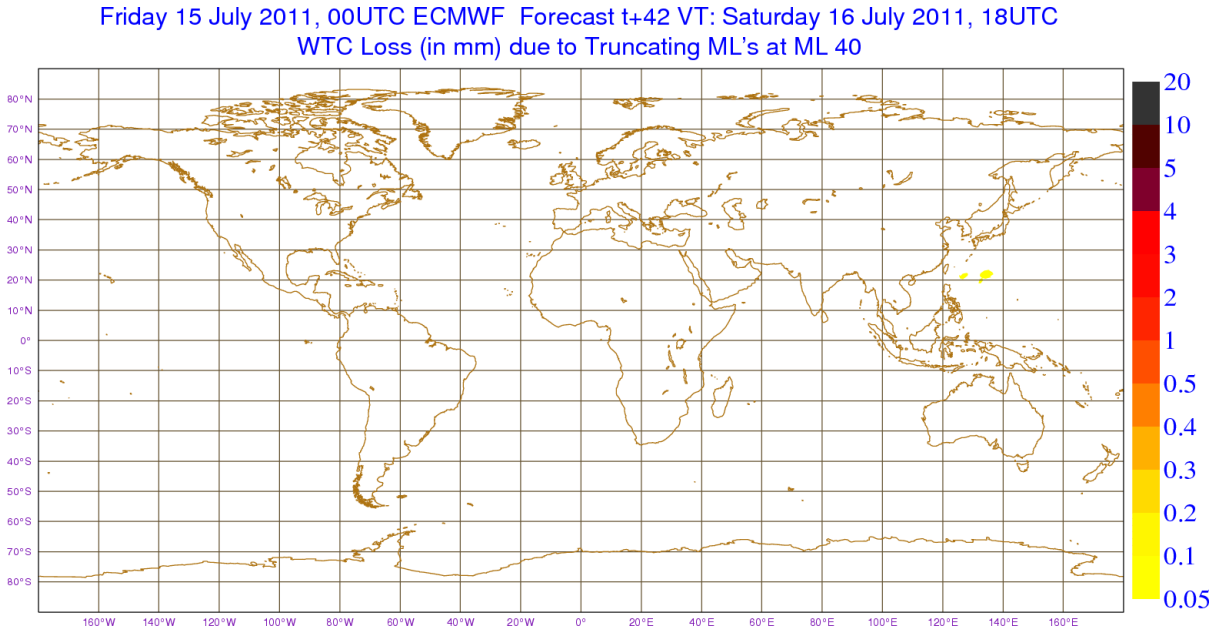

Figure 9: The WTC deficit (in mm) due to ignoring model levels higher than ML 40 (i.e. taking into account the lowest 52 model levels only) compared to considering all 91 model levels for the case of 42-hour forecast from 00 UTC on 15 July 2011 (valid at 18 UTC on 16 July 2011).

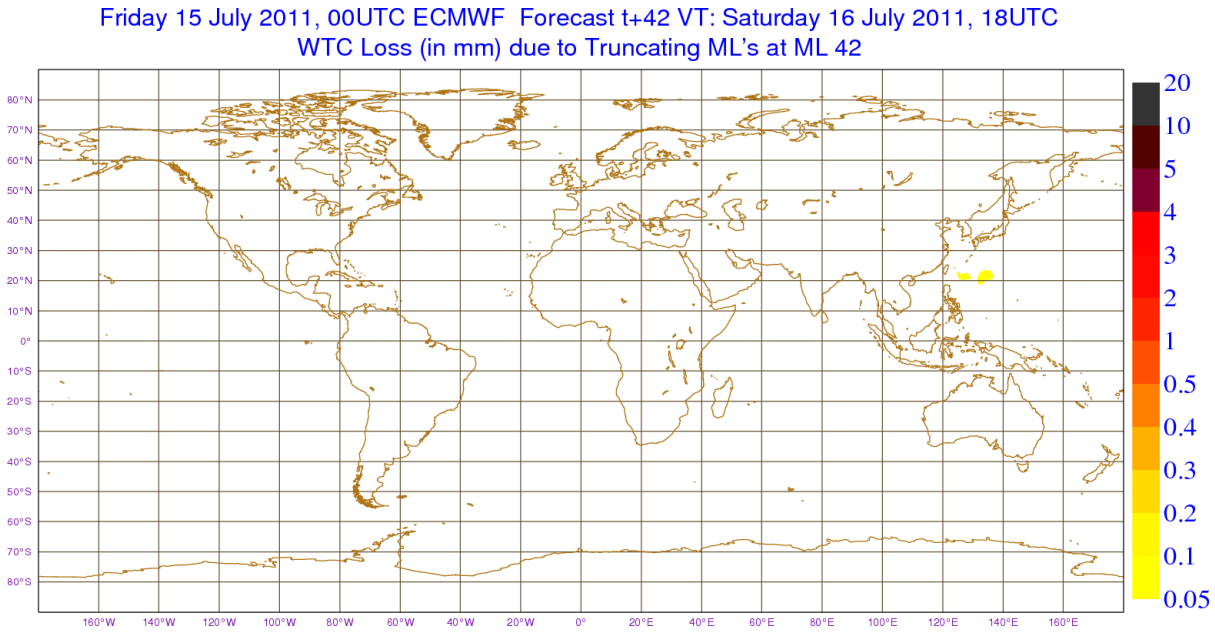

Figure 10: Same as Figure 9 but the truncation was done at ML 42 (i.e. taking into account the lowest 50 model levels only).

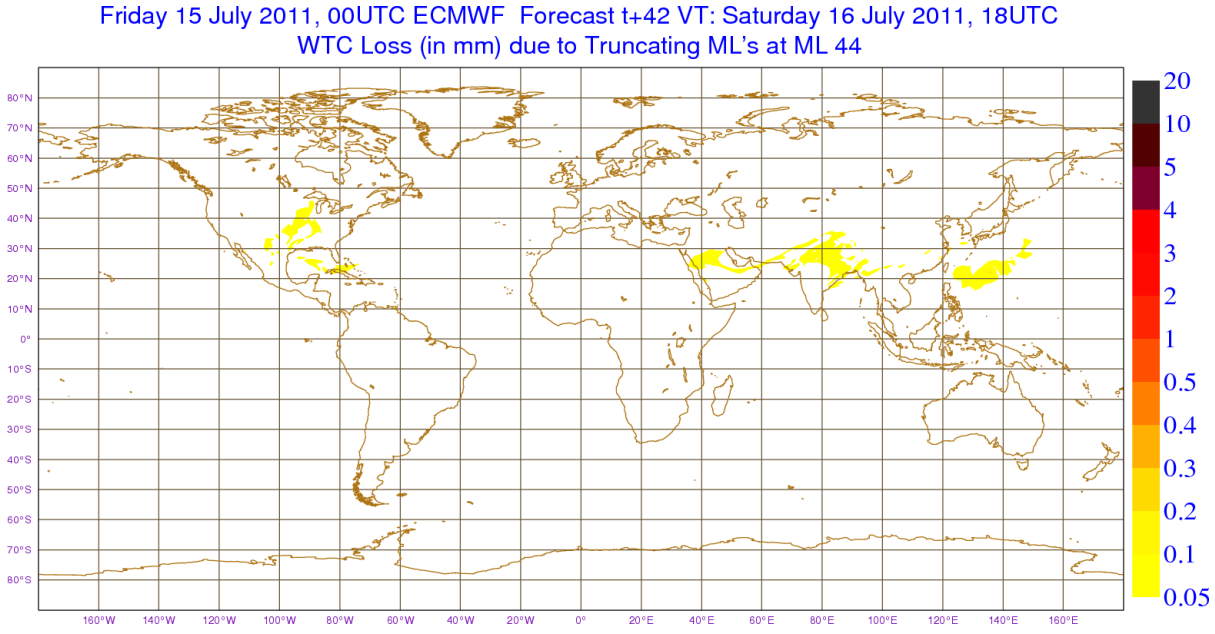

Figure 11: Same as Figure 9 but the truncation was done at ML 44 (i.e. taking into account the lowest 48 model levels only).

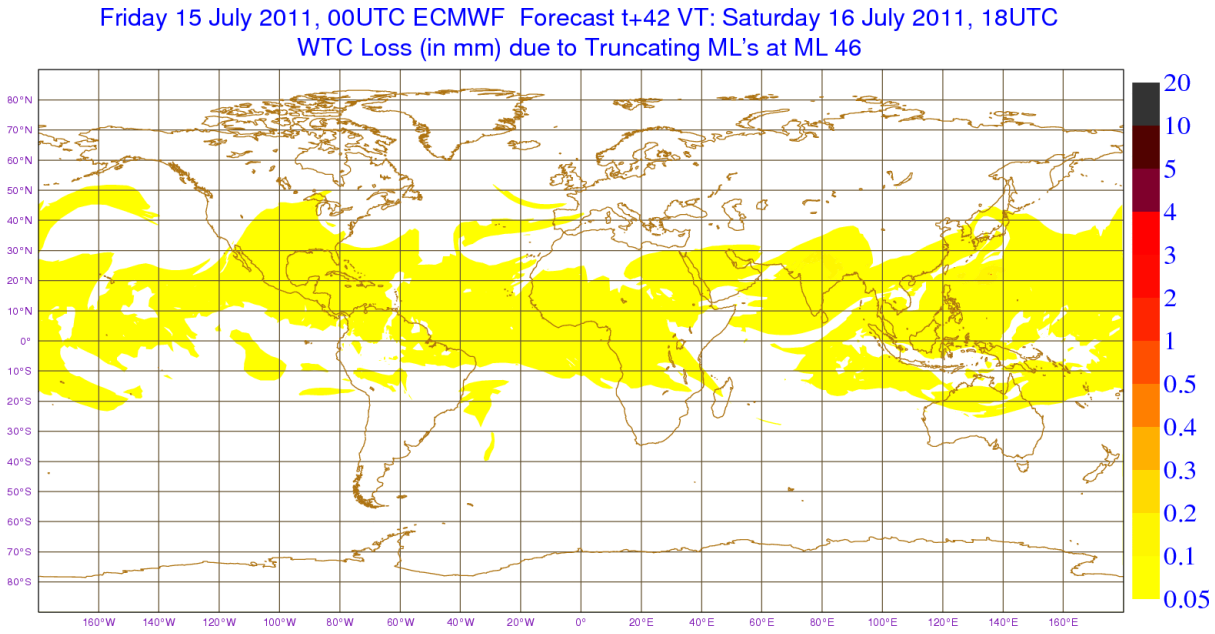

Figure 12: Same as Figure 9 but the truncation was done at ML 46 (i.e. taking into account the lowest 46 model levels only).

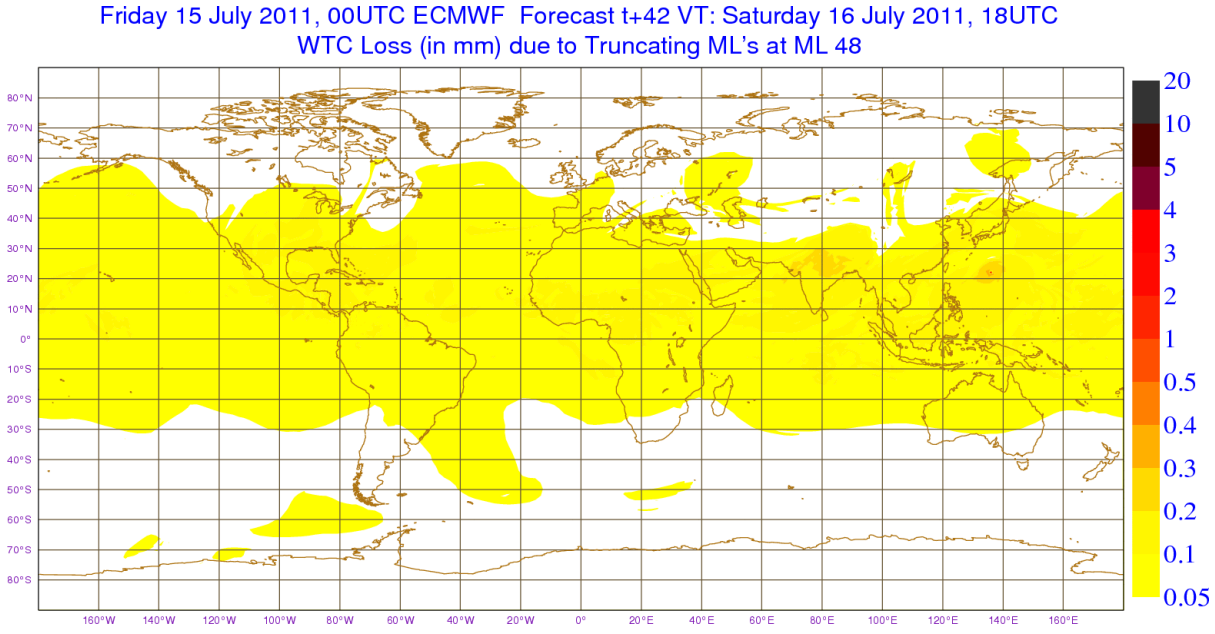

Figure 13: Same as Figure 9 but the truncation was done at ML 48 (i.e. taking into account the lowest 44 model levels only).

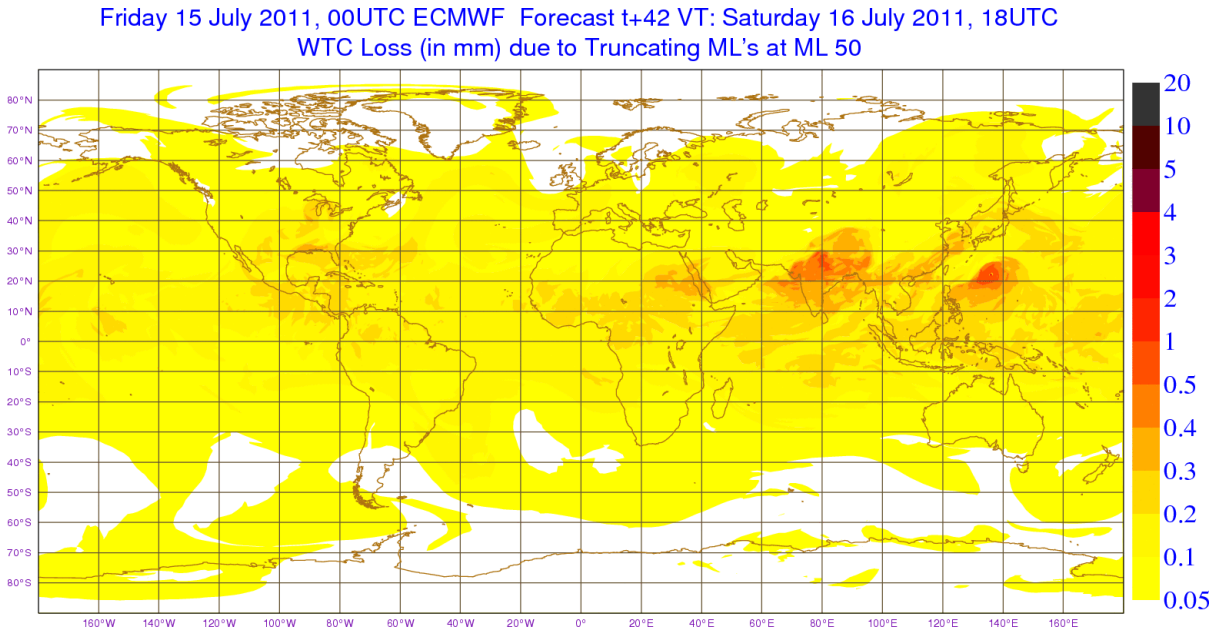

Figure 14: Same as Figure 9 but the truncation was done at ML 50 (i.e. taking into account the lowest 42 model levels only).

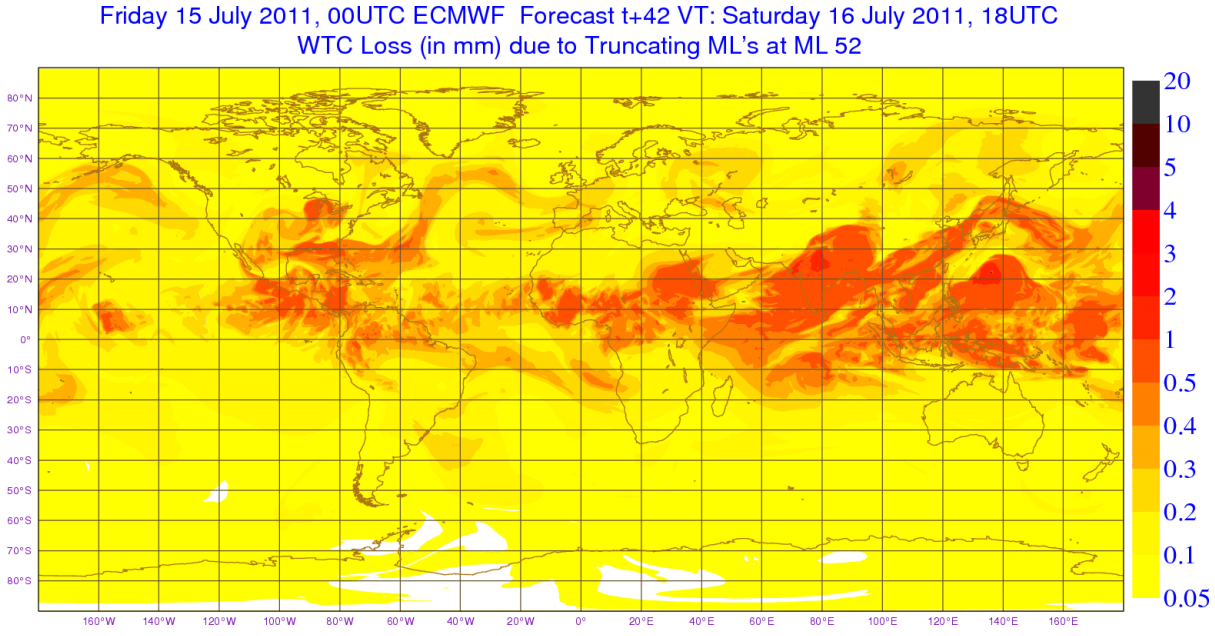

Figure 15: Same as Figure 9 but the truncation was done at ML 52 (i.e. taking into account the lowest 40 model levels only).

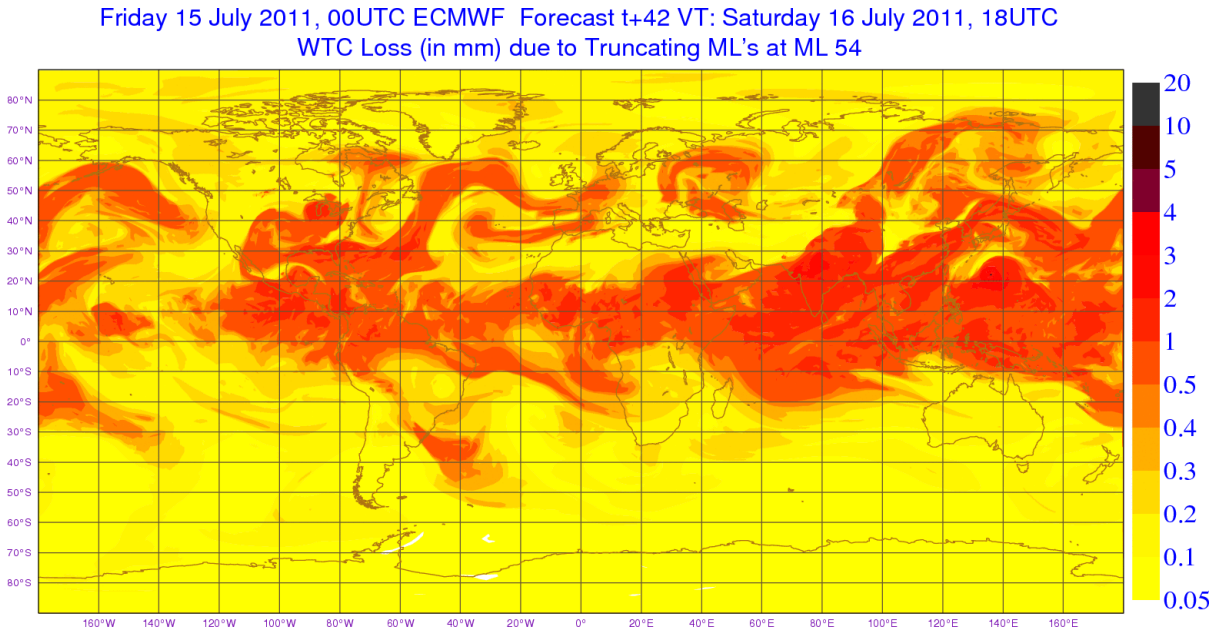

Figure 16: Same as Figure 9 but the truncation was done at ML 54 (i.e. taking into account the lowest 38 model levels only).

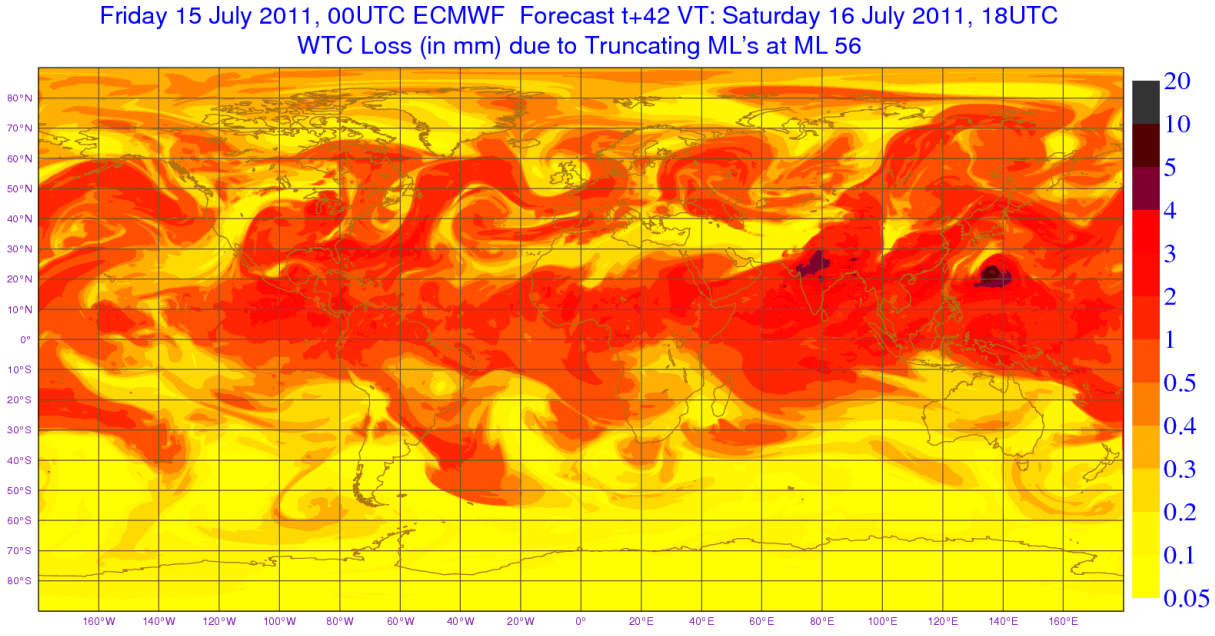

Figure 17: Same as Figure 9 but the truncation was done at ML 56 (i.e. taking into account the lowest 36 model levels only).

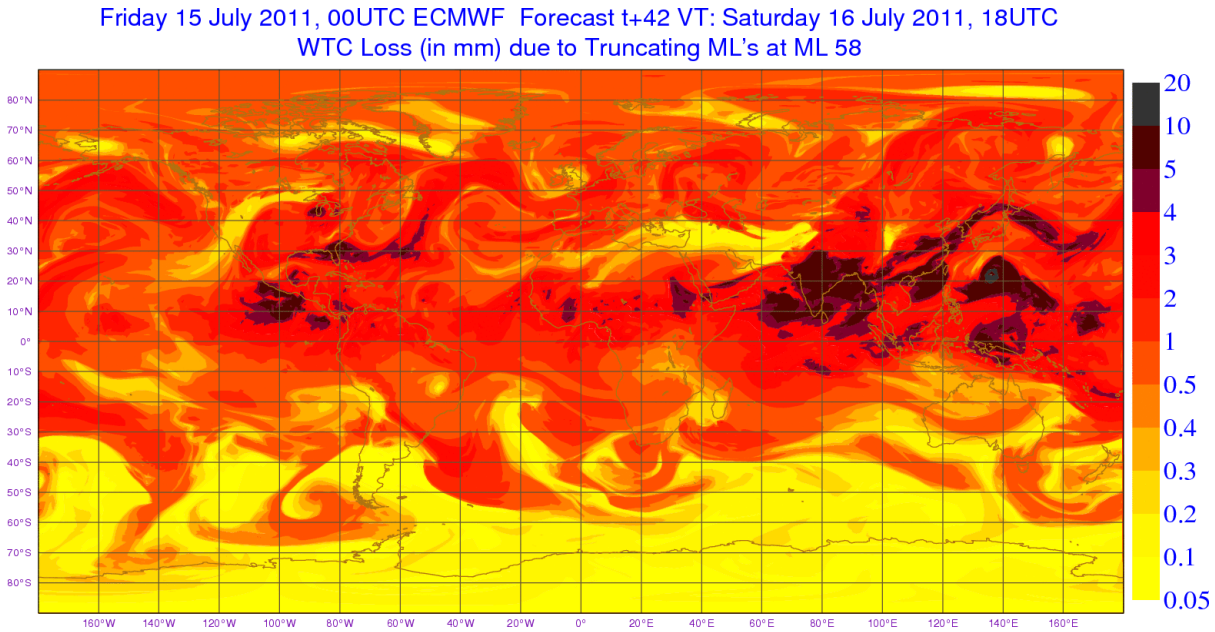

Figure 18: Same as Figure 9 but the truncation was done at ML 58 (i.e. taking into account the lowest 34 model levels only).

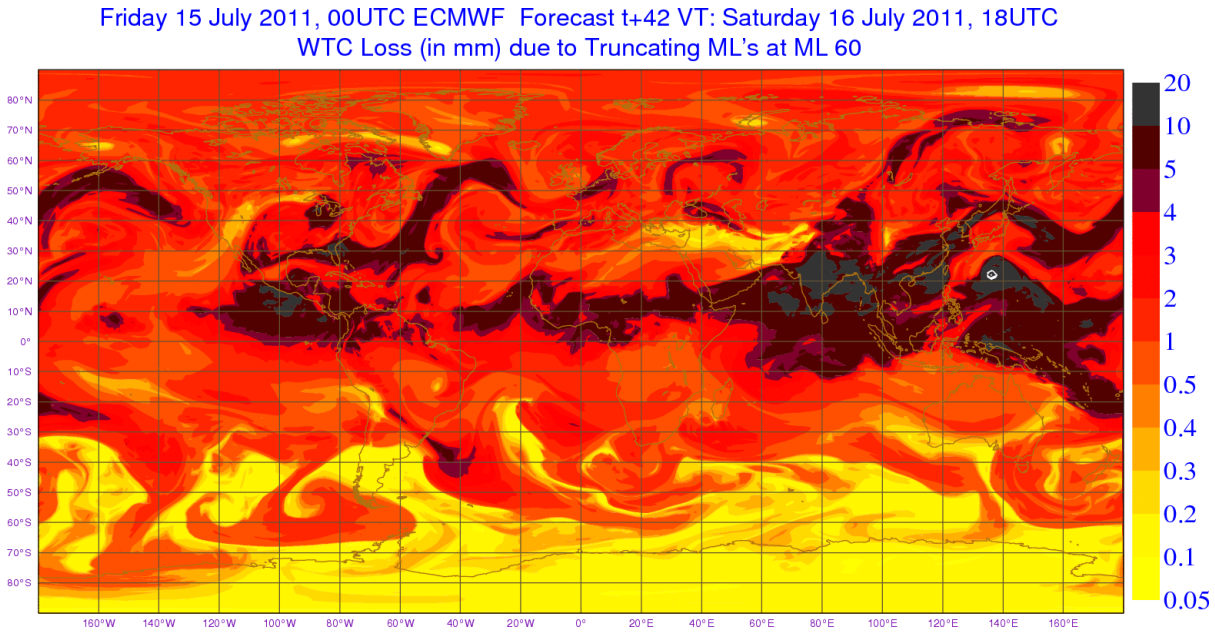

Figure 19: Same as Figure 9 but the truncation was done at ML 60 (i.e. taking into account the lowest 32 model levels only).

Figure 20 shows a close snapshot at the area with the largest WTC deficit due to truncation at ML 48 that corresponds to the global map of Figure 13. It is clear that the shape of the difference resembles a tropical cyclone. Records of tropical cyclones show that this is in fact "Ma-On Typhoon" which was active in mid July 2011 in that area (see, for example, NASA, 2011). The adverse impact of this typhoon on the truncated WTC computations can be reduced by including more model levels as can be seen in Figure 21, Figure 22 and Figure 23. The maximum deficit for that case reduces to about 3.4 mm, 1.4 mm and 0.2 mm if the truncation was done at ML 46, 44 and 42; respectively, as shown by the triangles in Figure 8. Based on the Tropical Rainfall Measuring Mission (TRMM) satellite measurements over the typhoon earlier that month (06:37 UTC on 11 July 2011 when the typhoon was still a tropical depression called "08W"), NASA (2011) found that the highest clouds were over 15 km high. This corresponds roughly to pressure of about 100 hPa or ML 40 (see the approximate conversion plot in Figure A1).

The other case with maximum WTC deficit around 1 mm in Figure 8 was found to be associated with the "Lau (16U) Cyclone" which was active in the mid of March 2012 in the Indian Ocean north-west of Australia. Again including 2 more model levels in the computations eliminate its adverse impact on the computations (not shown).

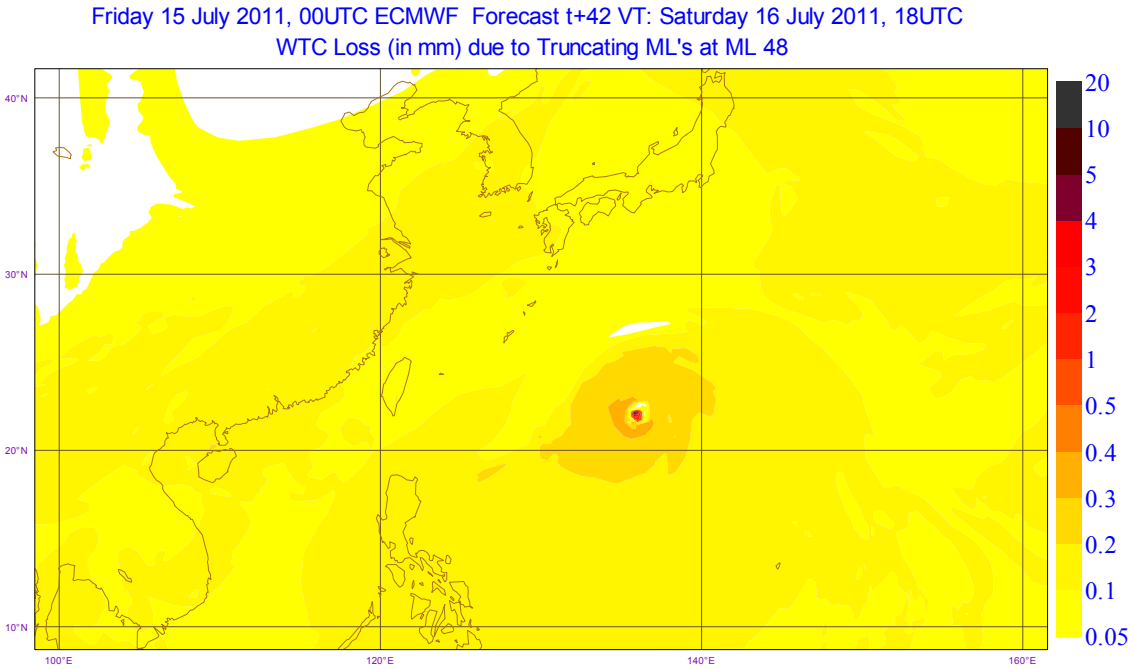

Figure 20: The WTC deficit (in mm) due to ignoring model levels higher than ML 48 (i.e. taking into account the lowest 44 model levels only) compared to considering all 91 model levels for the case of 42-hour forecast from 00 UTC on 15 July 2011 (valid at 18 UTC on 16 July 2011). This is a zoom of the Western Pacific region of Figure 13.

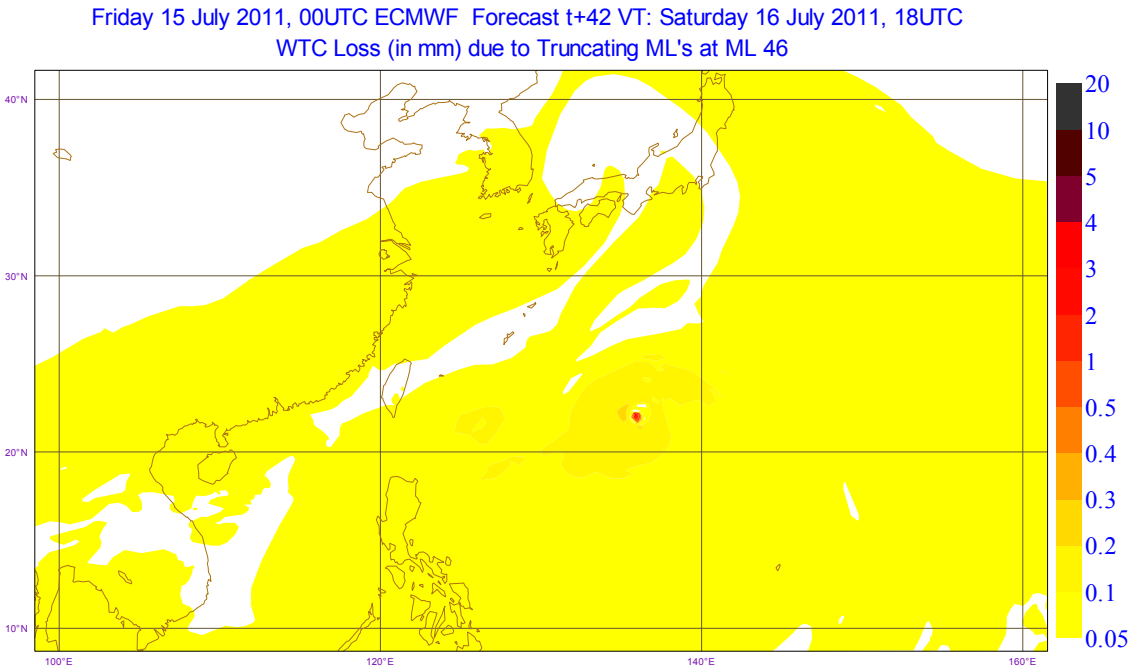

Figure 21: Same as Figure 20 but the truncation was done at ML 46 (i.e. taking into account the lowest 46 model levels only). This is a zoom of the Western Pacific region of Figure 12.

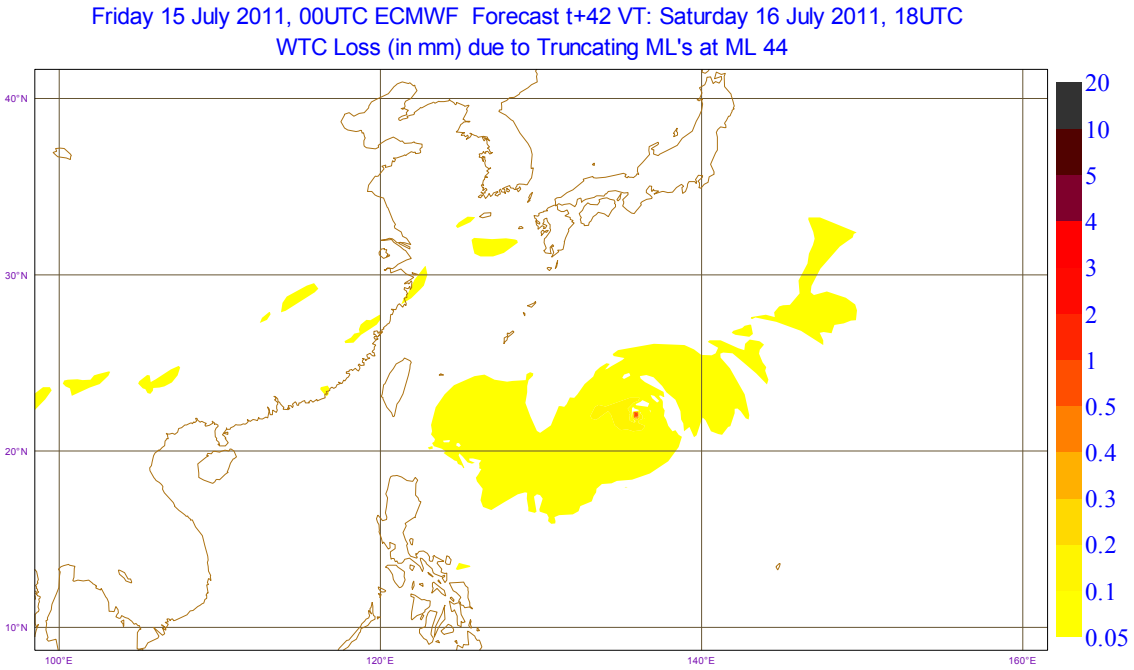

Figure 22: Same as Figure 20 but the truncation was done at ML 44 (i.e. taking into account the lowest 48 model levels only). This is a zoom of the Western Pacific region of Figure 11.

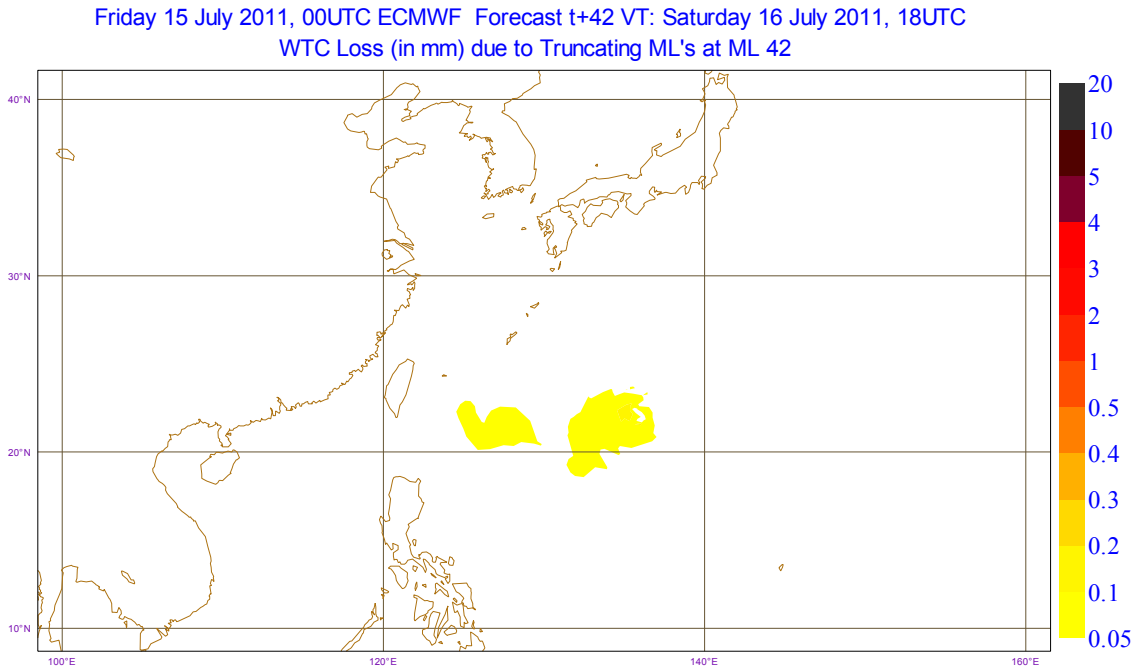

Figure 23: Same as Figure 20 but the truncation was done at ML 42 (i.e. taking into account the lowest 50 model levels only). This is a zoom of the Western Pacific region of Figure 10.

4.4. Extension of the Solution to 137 Model Levels

The ECMWF IFS model configuration was changed on 25 June 2013 to use 137 model levels. The results obtained in the previous section for the 91-ML configuration are verified for the case of the 137 ML's. As can be seen in Figure A1, model level number 48 (ML48) in the 91-ML model configuration corresponds to ML73 in the new 137-ML configuration.

A total of 154 cases from 1 January to 30 April 2013 were selected to sample the whole period, various hours of the day and various short-term forecasts (and analyses). The fields corresponding to those cases were extracted from the pre-operational model run (137-ML configuration). The WTC was computed by considering several level truncations. The results were compared to the WTC obtained from the integration of the whole atmospheric column (137 ML's) and the maximum deficits are shown as the family of continuous lines in Figure 24. For comparison, the corresponding fields from the operational model at the time (91-ML configuration) were also extracted and the very close model levels to those used in the 137-ML configuration were used for the truncation. The maximum deficit in each case are shown Figure 24 as a family of dashed lines. It is clear that the results of the case ML73 that considers only the lowest 65 ML's (i.e. levels 73 to 137) in the new model configuration correspond well with the case of ML48 in the old configuration. Even sometimes the new ML73 has slightly lower differences compared to old ML48. The maps of the differences look very similar (not shown).

Figure 24 shows that absolute maximum difference due to truncating at the new ML73 is within about 0.4 mm at all 154 cases except one (which is also corresponds to a tropical cyclone).

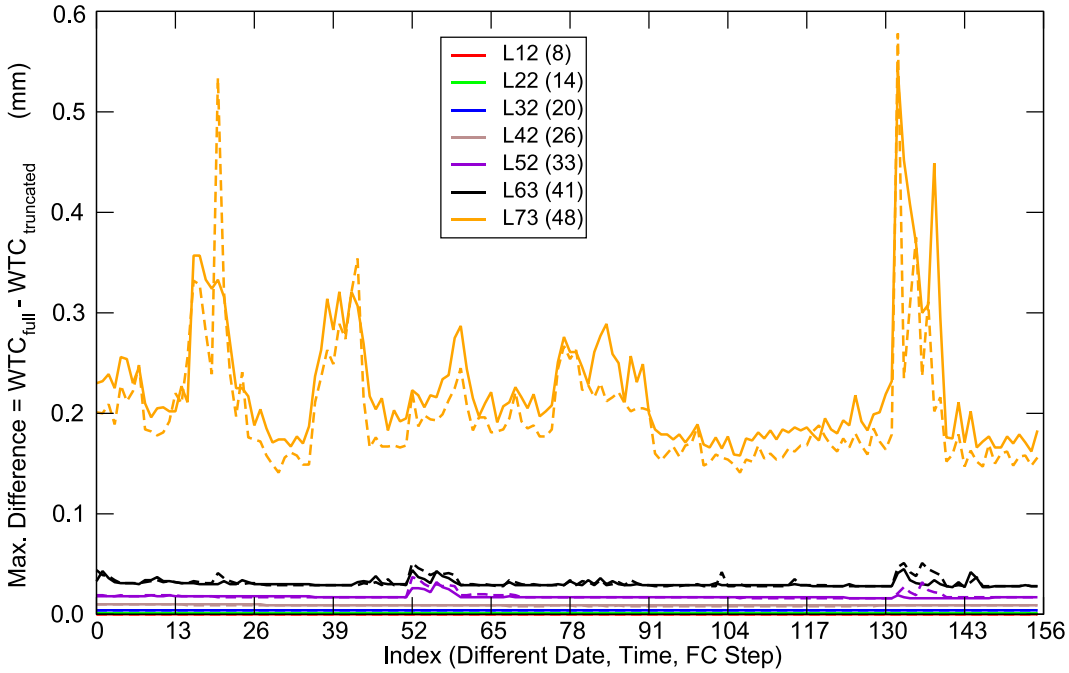

Figure 24: Maximum deficit due to truncating the WTC computations at various ML's (numbers after L corresponds to 137 ML's, while numbers between parentheses are corresponding 91 ML values) at each of the 154 cases from 1 January to 30 April 2013.

5. Conclusions

Computations of the dry tropospheric correction (DTC), which is the radar altimeter path delay due to the existence of the dry air, do not depend on the details of the atmospheric profile. Therefore, using model pressure-level (PL) fields does not deteriorate the results compared to the use of the model-level (ML) fields. While the maximum individual error in the considered 96 cases in first half of 2012 does not exceed 30 μm (30×10-6 m), the maximum mean over all the cases does not exceed 9 μm.

On the other hand, the computations of the wet tropospheric correction (WTC), which is the radar altimeter path delay due to the existence of the water vapour in the atmosphere, depend on the details of the atmospheric profiles. The limited number of pressure levels (around 25) is not enough to capture all the details of the humidity profiles especially in the tropical regions. Therefore, using the PL fields results into WTC deviations as high as 20 mm compared to the ML computations. The mean difference over the 96 cases considered in the first half of 2012 is as high as 4.5 mm. Considering the accuracy of the sea surface height measurements from radar altimeters, such differences are quite high. Therefore, PL fields cannot be recommended to be used for WTC.

Profiles of atmospheric humidity suggest that the specific humidity values at higher levels (above ~150-200 hPa) is about 3 orders of magnitude lower than its values at the lower levels. This fact can be implemented to ignore the uppermost "dry" layers of the atmosphere. Truncating the WTC computations at ML 48 (i.e. using the lowest 44 model levels only) in the 91-ML configuration and at

ML73 (i.e. using the lowest 65 model levels only) in the new 137-ML configuration result in mean differences not exceeding 0.16 mm and maximum individual differences not exceeding about 0.4 mm except at the locations of the tropical storms. Adding few more model levels would eliminate most of the errors at tropical storms. Old ML48 and new ML73 correspond to an elevation of about 12 km above the surface where the atmospheric pressure is about 185 hPa.

The possibility of achieving further savings by skipping some model levels was also considered but the errors were as high as the PL case (not presented here). However, further savings may be achieved by careful investigation of the humidity profiles to skip model levels with small vertical gradients. This is a time consuming task and therefore was not pursued.

Acknowledgements

The author would like to thank Peter Janssen and Agathe Untch for support and valuable discussions.

Appendix A: Conversion among model levels, pressure levels and altitude

Figure A1 provides a chart that can be used for crude conversion among current ECMWF model levels, pressure levels and altitudes from Earth surface. Several assumptions were used in order to produce this chart therefore it is only provided here as a guide to help the reader.

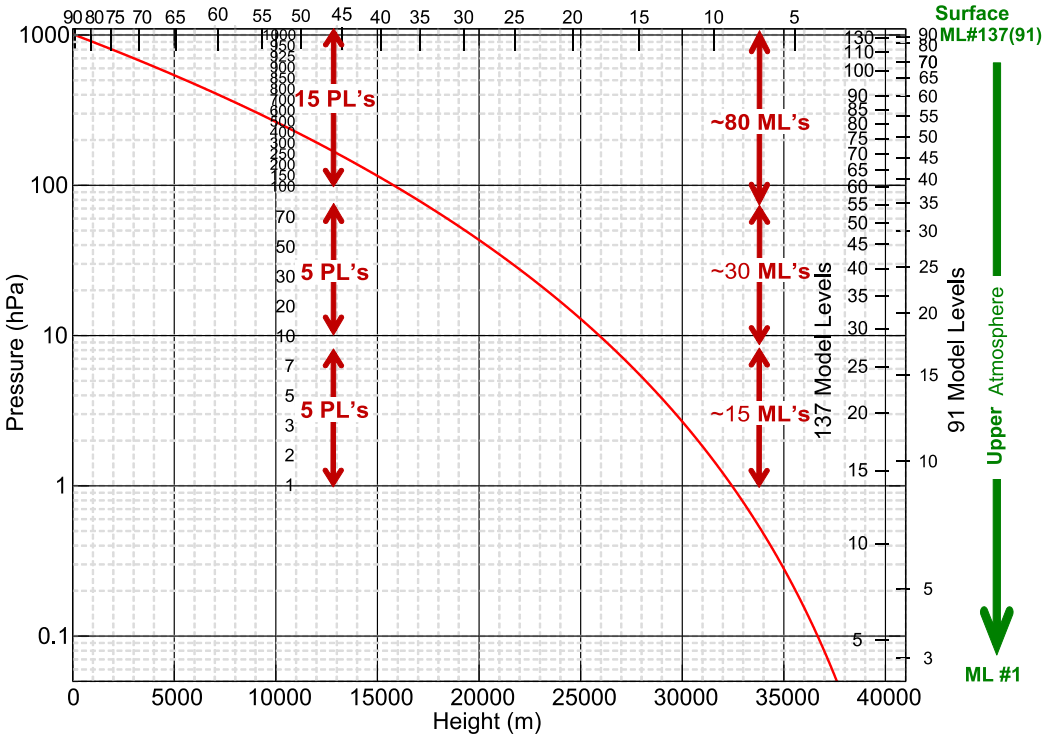

Figure A1: Approximate chart for crude conversion among ECMWF model levels (the 91- and 137-level model configurations), pressure levels and altitudes from Earth surface. Note that the upper x-axis and the outside of the right-hand side y-axis show the level numbers of the 91-level configuration while the inner side of the right-hand side y-axis shows the level number of the 137-level configuration.

Appendix B: Correspondence between 91 and 137 model level definitions

The correspondence between the model levels from the old operational ECMWF model (L91) and the new operational model since 25 June 2013 (L137) is given in ECMWF (2013). Table B1, which is copied from ECMWF (2013), shows the values of full level pressure, P_{L91} and P_{L137} for a surface pressure of 1013.250 hPa.

Table B1: The correspondence between the model levels from L91 and L137

L91		L137	
N_{L91}	P_{L91} [hPa]	N_{L137}	P_{L137} [hPa]
1	0.0100	1	0.0100
2	0.0299	2	0.0255
		3	0.0388
3	0.0568	4	0.0575
		5	0.0829
4	0.1015	6	0.1168
5	0.1716	7	0.1611
		8	0.2180
6	0.2768	9	0.2899
7	0.4285	10	0.3793
		11	0.4892
8	0.6396	12	0.6224
		13	0.7821
9	0.9244	14	0.9716
10	1.2985	15	1.1942
		16	1.4535
11	1.7781	17	1.7531
		18	2.0965
12	2.3800	19	2.4875
13	3.1209	20	2.9298
		21	3.4270
14	4.0176	22	3.9829
		23	4.6010
15	5.0860	24	5.2851
16	6.3417	25	6.0388
		26	6.8654
17	7.7988	27	7.7686
		28	8.7516
18	9.4706	29	9.8177
19	11.3688	30	10.9703
		31	12.2123
20	13.5037	32	13.5469
		33	14.9770
21	15.8844	34	16.5054
22	18.5179	35	18.1348
		36	19.8681
23	21.4101	37	21.7076
24	24.5653	38	23.6560
		39	25.7156
25	27.9860	40	27.8887
		41	30.1776
26	31.6736	42	32.5843
27	35.6281	43	35.1111
		44	37.7598
28	39.8481	45	40.5321
29	44.3310	46	43.4287
		47	46.4498
30	49.0732	48	49.5952
31	54.0701	49	52.8644
		50	56.2567
32	59.3150	51	59.7721
33	64.7978	52	63.4151
		53	67.1941
34	70.5061	54	71.1187
35	76.4292	55	75.1999
		56	79.4496
36	82.5725	57	83.8816
37	88.9589	58	88.5112
38	95.6172	59	93.3527
		60	98.4164
39	102.5813	61	103.7100
40	109.8913	62	109.2417
41	117.5942	63	115.0198
		64	121.0526
42	125.7453	65	127.3487
43	134.3981	66	133.9170
44	143.5909	67	140.7663
		68	147.9058
45	153.3538	69	155.3448
46	163.7180	70	163.0927

L91		L137	
N_{L91}	P_{L91} [hPa]	N_{L137}	P_{L137} [hPa]
47	174.7166	71	171.1591
		72	179.5537
48	**186.3837**	**73**	**188.2867**
49	198.7556	74	197.3679
		75	206.8078
50	211.8697	76	216.6166
51	225.7656	77	226.8050
52	240.4844	78	237.3837
		79	248.3634
53	256.0690	80	259.7553
54	272.5644	81	271.5704
55	290.0175	82	283.8200
		83	296.5155
56	308.4773	84	309.6684
57	327.9948	85	323.2904
		86	337.3932
58	348.6233	87	351.9887
59	370.4182	88	367.0889
		89	382.7058
60	393.4375	90	398.8516
61	417.7337	91	415.5387
		92	432.7792
62	443.3441	93	450.5858
63	470.1659	94	468.9708
		95	487.9470
64	497.9584	96	507.5021
65	526.4620	97	527.5696
66	555.3989	98	548.0312
		99	568.7678
67	584.4855	100	589.6797
68	613.4989	101	610.6646
		102	631.6194
69	642.2899	103	652.4424
70	670.7310	104	673.0352
71	698.7032	105	693.3043
		106	713.1631
72	726.0656	107	732.5325
73	752.6718	108	751.3426
		109	769.5329
74	778.4036	110	787.0528
75	803.1575	111	803.8622
76	826.8141	112	819.9302
		113	835.2358
77	849.2512	114	849.7668
		115	863.5190
78	870.3798	116	876.4957

L91		L137	
N_{L91}	P_{L91} [hPa]	N_{L137}	P_{L137} [hPa]
79	890.1341	117	888.7066
		118	900.1669
80	908.4403	119	910.8965
81	925.2226	120	920.9193
		121	930.2618
82	940.4415	122	938.9532
		123	947.0240
83	954.0914	124	954.5059
		125	961.4311
84	966.1707	126	967.8315
		127	973.7392
85	976.6735	128	979.1852
86	985.6311	129	984.2002
		130	988.8133
87	993.3027	131	993.0527
		132	996.9452
88	999.8373	133	1000.5165
89	1005.1222	134	1003.7906
		135	1006.7900
90	1009.1459	136	1009.5363
91	1012.0494	137	1012.0494

References

Cucurull, L., 2010. "Improvement in the Use of an Operational Constellation of GPS Radio Occultation Receivers in Weather Forecasting". *Wea. Forecasting*, **25**, 749-767.

ECMWF, 2011. "IFS documentation Cycle 37R2; Section 2.2.1: Vertical Discretization", a web page (last visited: 25 July 2012): http://www.ecmwf.int/research/ifsdocs/DYNAMICS/Chap2_Discretization4.html

ECMWF, 2013. "Model Level Definitions", a web page (last visited: 14 October 2013): http://www.ecmwf.int/products/data/technical/model_levels/index.html

Healy, S., 2009. "Refractivity coefficients used in the assimilation of GPS radio occultation measurements". GRAS SAF Report 09, SAF/GRAS/DMI/REP/GSR/009, http://www.grassaf.org

NASA, 2011. "Hurricane Season 2011: Tropical Depression Ma-On (Western No. Pacific Ocean)", a web page (last visited: 25 July 2012): http://www.nasa.gov/mission_pages/hurricanes/archives/2011/h2011_Ma-on.html

Rüeger, J., 2002. "Refractive index formulae for electronic distance measurements with radio and millimetre waves". University of New South Wales Unisurv Report, 68.